Med Biol Eng Comput (2006) 44: 511–515
DOI 10.1007/s11517-006-0052-2

TECHNICAL NOTE

Mateo Aboy · J. Haakon Falkenberg

An automatic algorithm for stationary segmentation of extracellular microelectrode recordings

Received: 18 October 2005 / Accepted: 22 March 2006 / Published online: 4 May 2006

Abstract Extracellular microelectrode recordings (MER) often contain artifact from a variety of sources that confound traditional signal-processing techniques that require stationary signal segments. We designed an algorithm to locate the longest stationary segment of MER signals. In this paper we provide a description of the segmentation algorithm and its performance assessment. Simulation results demonstrate that the automatic segmentation algorithm we proposed is capable of accurately identifying the boundaries of the longest stationary segments in MER signals. In our simulation study the segmentation algorithm correctly identified the boundaries of the longest MER stationary segments in 99.5% of the cases.

Keywords Extracellular microelectrode recording · MER segmentation · Monte Carlo simulation

1 Introduction

Parkinson's disease (PD) is the second most prevalent neurodegenerative disease and affects over 500,000 people in the USA and about 4–5% of people over 85 [3, 4]. Deep brain stimulation (DBS) of the internal segment of the globus pallidus (GPi) and the subthalamic nucleus (STN) have both shown to dramatically improve symptoms of PD and is increasingly being used for the treatment of advanced PD patients whose condition has deteriorated or who are no longer responsive to drug therapy. One of the critical challenges to neurosurgeons who perform stereotactic neurosurgery in PD patients is locating the target structure within the brain. Extracellular microelectrode recordings (MER) are commonly used during surgery to locate the STN and GPi targets because of its more precise target and physiological localization than MRI [6]. Despite the wide use of MER to locate the DBS targets and the dramatic clinical improvements of DBS, current methods of MER analysis still rely on manual techniques that are subjective, non-automatic, and cumbersome [1, 2, 5, 6]. During surgery the neurosurgeon typically analyzes the MER signals by examining the time–domain behavior of the signal on an oscilloscope (or equivalent) while listening to the signal through conventional speakers. Although modern surgical workstations provide some tools for MER signal semi-automatic analysis and processing, the techniques are cumbersome, need manual tuning, and require the neurosurgeon to mentally keep track of how the recordings change as the microelectrode moves through different brain structures. Furthermore, MER signals often contain artifact from a variety of sources such as patient movement and equipment noise. These sources confound signal processing and analysis techniques that require stationary signal segments.

In this paper we describe an automatic algorithm designed to identify the longest stationary segment in the input MER signal. The automatically selected segment can be considered to be the segment that most accurately represents the characteristics of the neural structure. This segment can be used for further automatic analysis such as power spectral density estimation and visualization.

Automatic segmentation of MER is of clinical significance because current pre- and post-operative analysis methods do not reliably remove artifacts automatically. Hence, automatic segmentation of MER shows promise in being pivotal as a tool needed for improving consistency and accuracy of MER analysis.

1.1 Problem formulation

Let $\boldsymbol{x} = (x_1, x_2, ..., x_N)^{\mathrm{T}}$ be an arbitrary MER signal composed of M locally wide sense stationary

M. Aboy (✉)
Department of Electronics Engineering Technology, Oregon Institute of Technology, Portland, OR 97006, USA
E-mail: mateoaboy@ieee.org

J. H. Falkenberg
University of Washington, Seattle, WA, USA

segments, $\{s\}_{l=1}^{M} = \{s_{1,N_1}, s_{2,N_2}, \ldots, s_{k,N_k}, \ldots, s_{M,N_M}\}$, where $\{N_l\}_{l=1}^{M}$ denotes the number of samples in each of the segments. The objective of MER segmentation is to select the segment s_{k,N_k} such that $N_k \geq \{N_l\}_{l=1}^{M}$. Practically, the duration of the selected segment τ_k is constrained to be longer than 3 s, since this is considered the shortest length necessary for the surgeon to reliably analyze a segment.

2 Algorithm description

The following sections describe our algorithm in a sequence of four steps.

2.1 Normalization and frame segmentation

The MER signal $\boldsymbol{x}$ is normalized by subtracting the mean and dividing by the standard deviation,

$$\boldsymbol{x_n} = \frac{\boldsymbol{x} - \mu_{\boldsymbol{x}}}{\sigma_{\boldsymbol{x}}}. \quad (1)$$

The normalized MER $\boldsymbol{x}_n$ is segmented into S non-overlapping frames $\{\boldsymbol{\chi}_l\}_{l=1}^{S}$ of equal time duration t,

$$\{\boldsymbol{\chi}_l\}_{l=1}^{S} = \{\boldsymbol{\chi}_1, \boldsymbol{\chi}_2, \ldots, \boldsymbol{\chi}_k, \ldots, \boldsymbol{\chi}_S\}. \quad (2)$$

The segment time duration t is user specified ($t > 3$ s).

2.2 Variance calculation

The autocorrelation sequence $r_x(l)$ is estimated for each of the frames $\{\boldsymbol{\chi}_k\}_{l=1}^{S}$ using the biased estimator of the autocorrelation $\hat{r}_x(l)$ in order to guarantee that the estimate is positive semi-definite. The variance of the covariance $\hat{\gamma}_x(l)$ is then estimated from $\hat{r}_x(l)$ for each frame $\boldsymbol{\chi}_k$ according to the following equation,

$$\mathrm{var}\{\hat{\gamma}_x(0)\} = \frac{2}{L}\sum_{l=-\infty}^{\infty}\hat{\gamma}_x^2(l) = \frac{2\sigma^4}{L}\sum_{l=-\infty}^{\infty}\hat{r}_x^2(l). \quad (3)$$

The variance of the covariance is used instead of the estimated sample variance or estimated variance of the sample variance because it does not assume independent observations. In the case of N independent normal observations, the variance of the sample variance $\hat{s}^2$ depends on σ and N,

$$\mathrm{var}\{\hat{s}^2\} \approx \frac{2\sigma^4}{N}. \quad (4)$$

Since $\{\boldsymbol{\chi}_l\}_{l=1}^{S}$ have equal duration, estimating the variance of the sample variance is equivalent to estimating the sample variance. However, when the samples cannot be assumed to be independent normal observations, N_i (the equivalent number of independent observations) is less than the number of samples in the segment ($N_i < N$) and Eq. 4 cannot be applied, i.e., the variance of the covariance takes into account the number of independent observations in a given segment $\boldsymbol{\chi}_k$. The output of this step is a vector with the variances of the autocovariances of $\{\boldsymbol{\chi}_k\}_{l=1}^{S}$, denoted $\boldsymbol{\upsilon}$,

$$\begin{aligned}\boldsymbol{\upsilon} &= \left[\mathrm{var}\left\{\hat{\gamma}_{\chi_1}(0)\right\}, \mathrm{var}\left\{\hat{\gamma}_{\chi_2}(0)\right\}, \ldots, \mathrm{var}\left\{\hat{\gamma}_{\chi_P}(0)\right\}\right]^{\mathrm{T}} \\ &= (\upsilon_1, \upsilon_2, \ldots, \upsilon_P)^{\mathrm{T}}\end{aligned}. \quad (5)$$

2.3 Sequential hypothesis testing

The algorithm uses a test statistic analogous to the classical F test for determining whether two random samples have equal variance,

$$\begin{aligned}\mathtt{F} &= \left(\frac{\upsilon_{N_1}}{\upsilon_{D_1}}, \ldots, \frac{\upsilon_{N_k}}{\upsilon_{D_k}}, \ldots, \frac{\upsilon_{N_{P-1}}}{\upsilon_{D_{P-1}}}\right)^{\mathrm{T}} \\ &= (\mathtt{F}_1, \mathtt{F}_2, \ldots, \mathtt{F}_k, \ldots, \mathtt{F}_{P-1})^{\mathrm{T}}\end{aligned} \quad (6)$$

$$\upsilon_{N_k} = \max\{\upsilon_k, \upsilon_{k+1}\}_{k=1}^{P-1} \quad (7)$$

$$\upsilon_{D_k} = \min\{\upsilon_k, \upsilon_{k+1}\}_{k=1}^{P-1} \quad (8)$$

The test statistic used to establish transition instances t_k is determined by calculating the ratios of the variances of the covariances for each two adjacent segments. The larger variance of the covariance values is placed in the numerator. When the test statistic $\mathtt{F}$ is greater than the critical value $\mathtt{F}_c$ the algorithm records a transition. Although the general form of this statistic is identical to that used in the classical F test, there are two important differences. First, in order to account for the temporal correlation present in neuronal signals, the variance of the autocovariance is used instead of the sample variance. Secondly, the critical value $\mathtt{F}_c$ was empirically calculated based on Monte Carlo simulations (i.e., $\mathtt{F}_c = 1.2$) as opposed to being calculated from a theoretical distribution based on the degrees of freedom.

2.4 Segment selection

From the transition instances t_k the algorithm constructs a vector $\boldsymbol{t} = (t_1, t_2, ..., t_{M+1})^{\mathrm{T}}$ and the element by element differences $\nabla\boldsymbol{t}$,

$$\nabla\boldsymbol{t} = (\boldsymbol{t_2} - \boldsymbol{t_1}, \ldots, \boldsymbol{t_{m+1}} - \boldsymbol{t_m}, \ldots, \boldsymbol{t_{M+1}} - \boldsymbol{t_M})^{\mathrm{T}}. \quad (9)$$

The longest wide stationary segment ($\boldsymbol{s_{k,N_k}}$ such that $N_k \geq \{N_i\}_{l=1}^{M}$) is selected from $\nabla\boldsymbol{t}$,

$$\boldsymbol{s_{k,N_k}} = \arg\max_{\boldsymbol{m}} \nabla\boldsymbol{t}. \quad (10)$$

3 Performance assessment

With real MER signals there is no gold standard that can be used to assess the accuracy of automatic segmentation algorithms. In order to overcome this limitation, we designed a nonstationary MER signal synthesizer intended to be used in MER segmentation applications based on an statistical model of MER signals. The algorithm was assessed quantitatively on synthetic MER signals.

We modeled nonstationary MER signals $\boldsymbol{x} = [x_1, x_2, ..., x_N]^T$ as a progression of locally stationary segments $\{s\}_{l=1}^{M} = \{s_{1,N_1}, s_{2,N_2}, \ldots, s_{k,N_k}, \ldots, s_{M,N_M}\}$. Each stationary segment of the MER signal was approximated by an p-th order autoregressive process AR(p). A block diagram of the MER synthesis system is given in Fig. 1a. A set of white Gaussian noise signals of different time durations τ is generated by a random number generator. The time duration is determined by a Poisson random variable with mean λ. Each white Gaussian signal is then multiplied by a uniformly distributed random variable $\sqrt{(\sigma)} \sim U(0,1)$. The result is a set of white Gaussian random signals $\{\boldsymbol{w}_l\}_{l=1}^{M}$, each with a different variance σ and time duration τ. Each $\boldsymbol{w}_l$ is passed through a synthesis or coloring filter $H(z)$ to introduce dependence in the white noise input,

$$H(z) = \frac{1}{A(z)} = \frac{1}{1 + \sum_{k=1}^{P} a_k z^{-k}}. \tag{11}$$

The model parameters $\{a_l\}_{l=1}^{P} = (a_1, a_2, ..., a_P)$ and the model order P were estimated from MER signals in order to match the second order statistics of real MER signals. We used two representative sets of MER signals

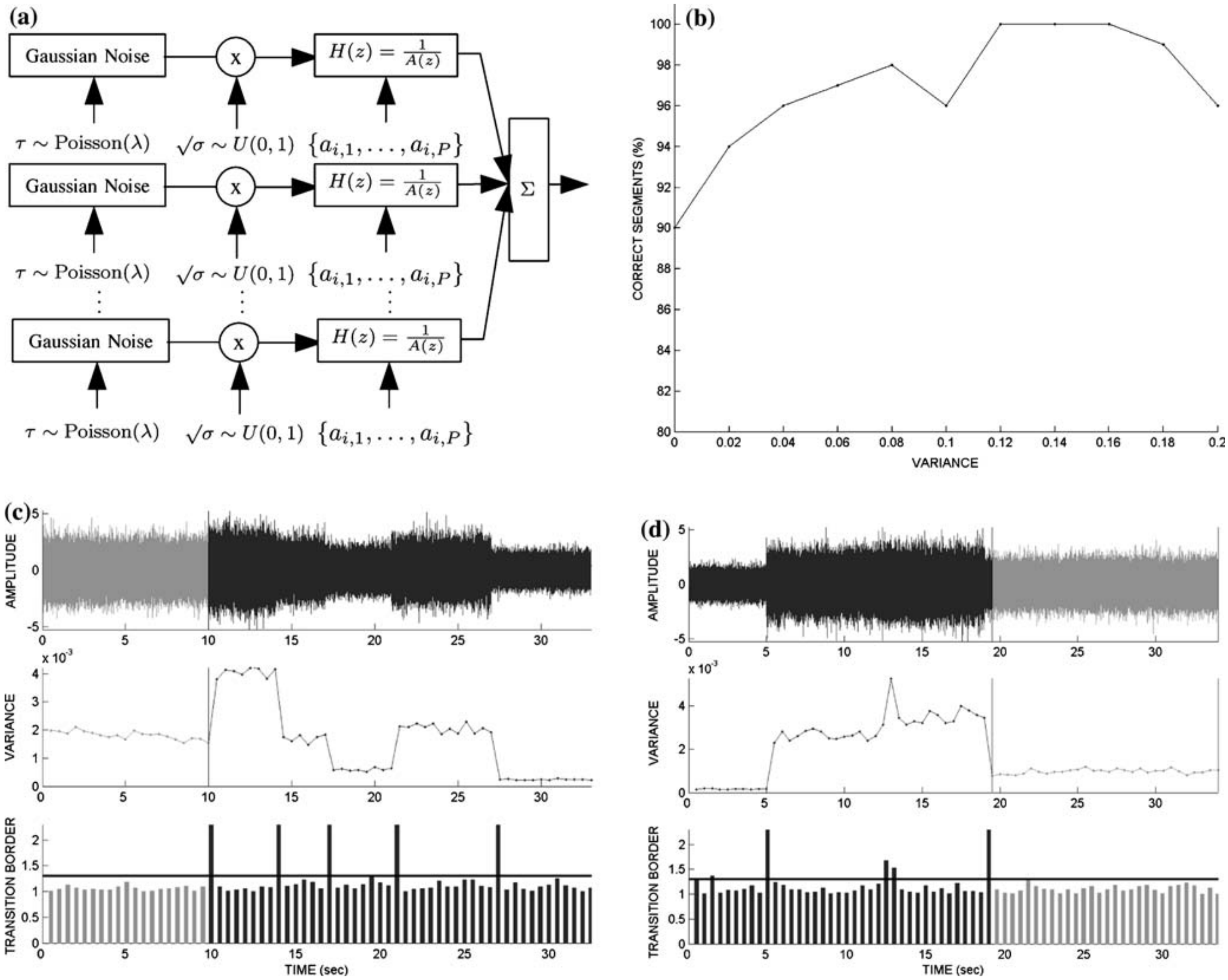

Fig. 1 Illustration of the segmentation process performed by the algorithm on synthetic MER signals with different transition times. **a** Block diagram of the MER signal simulator. **b** Algorithm's performance as a function of the minimum variance difference between two adjacent segments. **c** The *top plot* shows a synthetic MER signal with transitions at 10, 14, 17, 21, 27 (given by the MER simulator). The *middle plot* shows the variance of the autocovariance calculated by the segmentation algorithm, and the *plot* at the *bottom* shows the transition borders detected by the algorithm using a critical value of 1.2. The selected segment is shown in light *gray*. **d** Example of segmentation process performed by the algorithm on a synthetic MER signal with transition times equal at 5, 12, 19, 26

from two different patients to estimate the model parameters of each region and constructed a 10×50 matrix $\mathbf{A}$ containing two rows for each of the 5 brain regions, each row consisting of 50 model parameters,

$$\mathbf{A} = \begin{pmatrix} a_{1,1} & a_{1,2} & \cdots & a_{1,50} \\ a_{2,1} & a_{2,2} & \cdots & a_{2,50} \\ \vdots & \vdots & \ddots & \vdots \\ a_{10,1} & a_{10,2} & \cdots & a_{10,50} \end{pmatrix}. \tag{12}$$

Since segmentation must be performed on MER signals from all the five different brain regions, the simulator selects randomly a row of the matrix $\mathbf{A}$ each time it has to synthesize a signal. The five different MER regions estimated were reticular thalamus (RT), zona incerta (ZI), fields of forel (FF), STN, and substantia nigra reticulata (SNR). These five different regions are typically all encountered during stereotactic DBS surgery in the STN. The stationary segments $\{\mathbf{s}\}_{l=1}^{M}$ drawn from different distributions are concatenated to generate the realizations of nonstationary MER.

The model parameters $\{a_l\}_{l=1}^{P} = (a_1, a_2, \ldots, a_P)$ were estimated considering both forward and backward predictors and minimizing the combined error,

$$\varepsilon_P^{fb} = \sum_{n=N_i}^{N_f} \left[|e^f(n)|^2 + |e^b(n)|^2 \right] \tag{13}$$

$$\varepsilon_P^{fb} = \sum_{N_i}^{N_f} \left[|\hat{\mathbf{a}}^H \mathbf{x}(n)^2| + |\hat{\mathbf{a}}^H \mathbf{x}^*(n)|^2 \right], \tag{14}$$

where the first element of $\hat{\mathbf{a}}$ is 1. The minimization of the combined error results in a set of normal equations, which can be solved efficiently to obtain the model parameters.

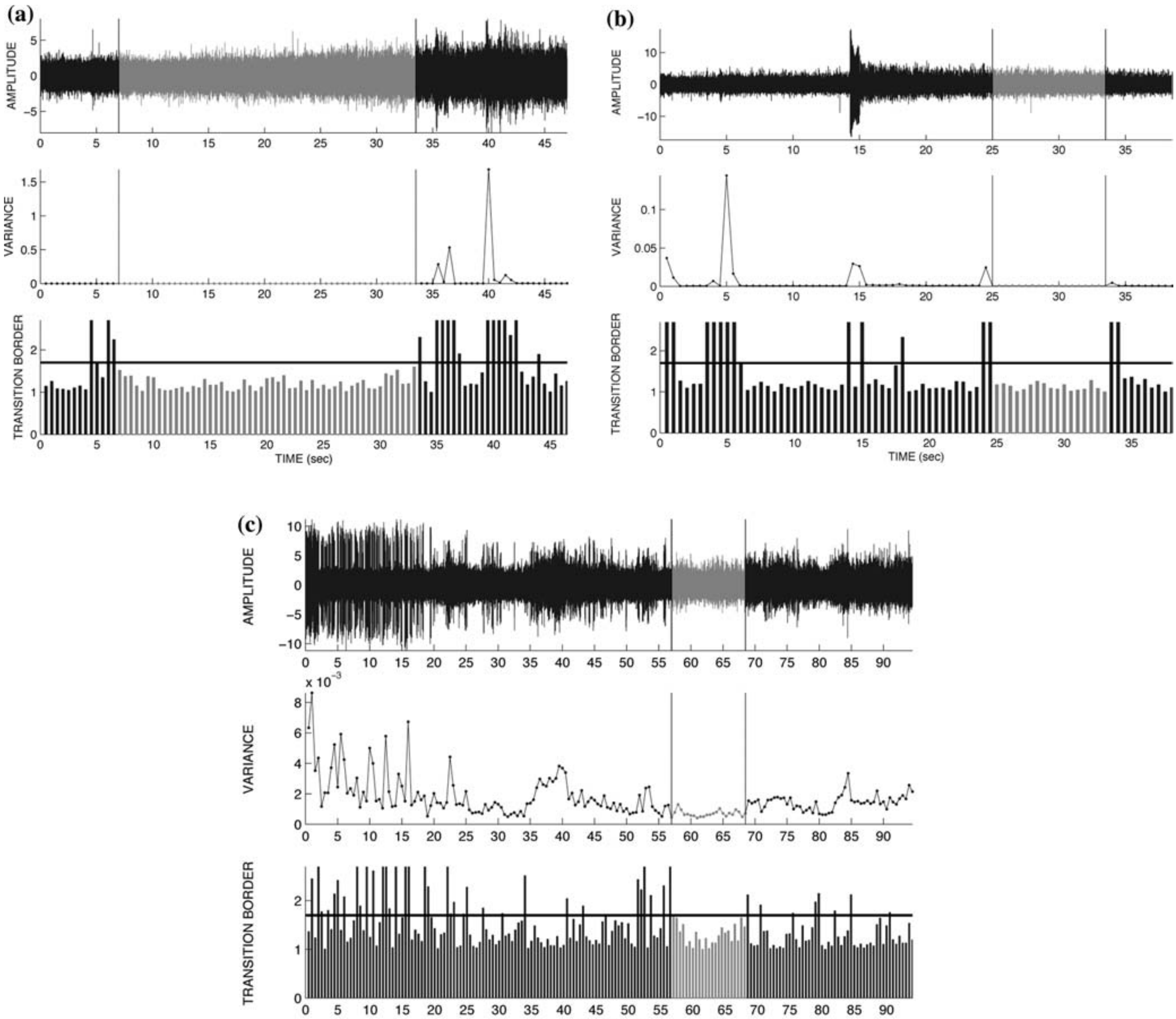

Fig. 2 Demonstration of automatic stationary segmentation of real MER signals using the proposed segmentation algorithm

Figure 1c, d illustrates the segmentation process performed by the segmentation algorithm in two different synthetic realizations of MER.

A simulation was performed in order to determine the optimal critical value for F_c. The objective of this simulation study was optimized to the algorithm's performance as a function of F_c. The value of F_c was incremented from 1 to 2 in steps of 0.01. For each F_c, we synthesized 1,000 MER signals, applied the segmentation algorithm, and evaluated its performance. The performance was defined as the number of times the algorithm selected the correct segment divided by 1,000. Based on this simulation we concluded that $F_c = 1.2$ results in the best performance.

In order to assess the algorithm we performed a simulation study to determine the minimal variance between two segments that was correctly differentiated as a transition instant (i.e., resolution). The MER simulator was used to generate the synthetic MER signals for this study. We evaluated the algorithm's performance by incrementing the value of σ_m from 0.001 to 0.2. Figure 1b shows the performance of the algorithm as a function of the minimum variance difference allowed between two adjacent segments (resolution). The plots show an algorithm performance close to 100% for resolutions as low as 0.1.

In addition to assessing the algorithm on synthetic MER signals, we tested the algorithm on real MER signals. Figure 2a–c show three representative examples demonstrating the segmentation performed by the algorithm on real MER signals. These three examples of segmentation of real MER signals where chosen because the segmentation was particularly difficult due to the small variance changes between the segments.

4 Conclusions

We described an automatic stationary segmentation algorithm for MER signals. The algorithm was assessed using synthetic MER signals. The simulation study performed on synthetic MER signals showed that the algorithm was capable of locating the longest stationary segment 99.5% of the time. We showed representative examples where the proposed automatic algorithm segmenting synthetic and real MER signals. The proposed automatic algorithm enables to locate the longest stationary segment present in the MER signal more objectively and faster than the current manual techniques based on visual inspection. Automatic segmentation algorithms are of significant clinical relevance because more objective, consistent and universal standards are needed to improve selection of optimal targets for DBS implantation and ablation, while minimizing microelectrode recording and surgery time, cost and possible surgical complications.

References

1. Burchiel KJ, Anderson VC, Favre J, Hammerstad JP (1999) Comparison of pallidal and subthalamic nucleus deep brain stimulation for advanced Parkinson's disease: results of a randomized, blinded pilot study. Neurosurgery 45(6):1375–1384
2. Favre J, Taha JM, Baumann T, Burchiel KJ (1999) Computer analysis of the tonic, phasic, and kinesthetic activity of pallidal discharges in Parkinson patients. Surg Neurol 51:665–673
3. Lang AE, Lozano AM (1998) Parkinson's diease. First of two parts. N Engl J Med 339:1044–1053
4. Lang AE, Lozano AM (1998) Parkinson's diease. Second of two parts. N Engl J Med 339:1130–1143
5. Vitek JL, Bakay RA, Hashimoto T, Kaneoke Y, Mewes K, Zhang JY, Rye D, Starr P, Baron M, Turner R, DeLong MR (1998) Microelectrode-guided pallidotomy: technical approach and its application in medically intractable Parkinson's disease. J Neurosurg 88:1027–1043
6. Zonenshayn M, Rezai AR, Mogilner AY, Beric A, Sterio D, Kelly PJ (2000) Comparison of anatomic and neurophysiological methods for subthalamic nucleus targeting. Neurosurgery 47(2):282–294